

Research Article

A Facile Synthesis of $\text{La}_2\text{O}_3/\text{GO}$ Nanocomposites in N,N-Dimethylformamide with High Dye Degradation Efficiency

Yong Wu He , Yao Bing Yin, Tao Chang , Li Bian ,
Guang Qing Zhang , and Xiao Liang Li 

College of Materials Science and Engineering, Hebei University of Engineering, Handan 056038, China

Correspondence should be addressed to Guang Qing Zhang; zhangqq0201@126.com and Xiao Liang Li; lixiaoliang@hebeu.edu.cn

Received 30 November 2017; Revised 21 January 2018; Accepted 18 February 2018; Published 26 March 2018

Academic Editor: Xuping Sun

Copyright © 2018 Yong Wu He et al. This is an open access article distributed under the Creative Commons Attribution License, which permits unrestricted use, distribution, and reproduction in any medium, provided the original work is properly cited.

La_2O_3 /graphene oxide (GO) nanocomposites were simply synthesized from commercially available $\text{LaCl}_3 \cdot 7\text{H}_2\text{O}$ and multilayer GO (5–10 layers) in N,N-dimethylformamide (DMF) under reflux condition without extra stabilizer. The characterization results of scanning electron microscopy (SEM), transmission electron microscopy (TEM), and X-ray photoelectron spectrum (XPS) spectroscopies showed that the crystalline La_2O_3 nanoparticles were successfully attached on the surface of GO. Moreover, the as-prepared nanocomposites greatly enhanced the degradation efficiency of organic dyes after 15 min under ultrasound irradiation in pure water. The degradation efficiency of the nanocomposites for methylene blue could be over 99%.

1. Introduction

Owing to their great catalytic, mechanical, magnetic, and optoelectronic properties, the synthesis of graphene oxide- (GO-) based nanocomposites has received great attention in recent decade [1]. Therefore, many kinds of GO-nanoparticle composites have been prepared by decorating GO with the nanoparticles such as Au [2], Pt [3], Ag [4], Ni [5], Fe_3O_4 [6], MnO_2 [7], NiO [8], and TiO_2 [9]. Up to now, however, GO nanocomposites based on the hybridization with rare earth oxides are relatively rare. Lanthanum oxide nanoparticles, one of the rare earth oxides, have been exploited for application in many interesting fields [10–14]. And more recently Chen group [15] reported removal of phosphate with graphene-lanthanum composite. However, the composite was obtained in two steps: synthesizing La_2O_3 particles and then mixing with GO to produce the composite. Hence, it is still necessary to develop new method for synthesis of $\text{La}_2\text{O}_3/\text{GO}$ nanocomposites.

In this work, $\text{La}_2\text{O}_3/\text{GO}$ nanocomposites were simply prepared from the commercially available $\text{LaCl}_3 \cdot 7\text{H}_2\text{O}$ and GO in DMF without extra stabilizer in one step. And the as-prepared products were characterized by SEM, TEM, and XPS. Moreover, the nanocomposites showed excellent

efficiency for methylene blue (MB), rhodamine B (Rh), and methyl orange (MO) degradation in water under ultrasound for 15 min.

2. Materials and Methods

Multilayer GO (5–10 layers) was purchased from Hengqiu Graphene Technology (Suzhou, China) and all other chemical reagents were of analytical grade and used as received without further purification. SEM images were obtained on Hitachi JSM-6360LV equipped with an energy dispersive X-ray spectroscopy. TEM investigations were performed on JEOL JEM 1200EX. XPS were obtained on Thermo Escalab 250Xi. UV-Vis spectrum was recorded on Beijing Persee TU-1810. Sonication was performed on ShenZhen JieMeng JP-010T ultrasonic cleaner with a frequency of 40 KHz and a nominal power of 100 W.

Preparation procedure: 0.050 g multilayer GO was added to 50 mL DMF and sonicated for 1 h. Then different amount of $\text{LaCl}_3 \cdot 7\text{H}_2\text{O}$ (0.050 g, 0.100 g, and 0.150 g) was added and the whole mixtures were stirred under reflux condition for 1 h. The synthesized nanocomposites were collected by centrifugation and washed three times with distilled water

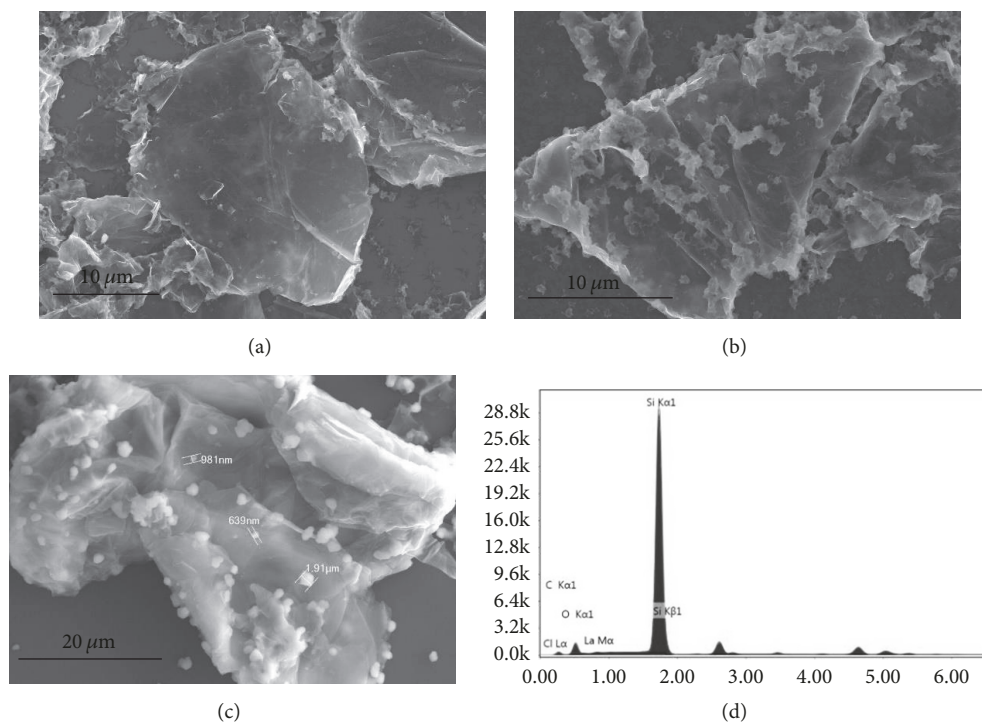


FIGURE 1: SEM images of (a) GL1, (b) GL2, (c) GL3, and (d) EDX spectrum of GL3.

and ethanol and then dried in a vacuum oven at 60°C overnight and labeled as GL1, GL2, and GL3, respectively.

Dye degradation procedure: the GL1, GL2 and GL3 nanocomposites were dispersed in distilled water and sonicated for 30 min to give 1 mg/mL suspension, respectively. The 0.2 mL as-prepared suspensions were added to rhodamine B, methylene blue, and methyl orange solutions in water (50 mL, 10^{-6} mol/L), respectively, and the all mixtures irradiated under ultrasound for 15 min. After centrifugation, the UV-vis spectra of the supernatants were recorded for calculation of dye degradation efficiency.

3. Results and Discussion

The $\text{La}_2\text{O}_3/\text{GO}$ nanocomposites were synthesized by using $\text{LaCl}_3 \cdot 7\text{H}_2\text{O}$ and GO in DMF under reflux condition in one step. As shown in Figure 1(a), the SEM image of GL1 showed that only a few of spherical nanoparticles could be observed on GO surface. In addition, more and larger nanoparticles could be observed in Figures 1(b) and 1(c) for GL2 and GL3, respectively, because of increasing the concentration of $\text{LaCl}_3 \cdot 7\text{H}_2\text{O}$. The above results indicated that particle size of La_2O_3 on GO surface could be enlarged as increasing the concentration of La^{3+} in the mixture. In addition, EDX spectra were also studied in Figure 1(d), which confirmed that lanthanum could be successfully attached on the surface of nanocomposites.

TEM images of GL2 in Figure 2 showed the morphology of the $\text{La}_2\text{O}_3/\text{GO}$ nanocomposites. As shown in Figure 2(a), a few of the La_2O_3 nanoparticles were aggregated which could

be also observed in SEM images. And the average size of the most La_2O_3 nanoparticles on GO sheets was estimated to be approximately 8 nm with a narrow size distribution of 4–19 nm. Moreover, most of the La_2O_3 nanoparticles were found on the surface of GO sheets and almost no free nanoparticles were observed, which indicated the strong interaction between La_2O_3 nanoparticles and GO sheets. Similarly, the same phenomena could be found in TEM images of GL1 and GL3, respectively. And in order to study the function of GO in the formation of the nanocomposites, the controlled experiment was carried out in absence of GO (Supplementary Materials (available here)). Some white solid could also be obtained in DMF without GO; however, most of the particles were aggregated according to the TEM images (Figure S1). The result suggested that GO could not only be used as a template or substrate with a large surface area for anchoring nanomaterials, but also prohibit the aggregation of nanoparticles [4]. Moreover, the component of the solid was studied by XRD. According to the XRD spectra (Figure S1C), the solid may contain some $\text{La}(\text{OH})_3$, but most of the solid was complex of lanthanum with DMF. All the results indicated that the GO played a significant role in the synthesis of La_2O_3 nanoparticles, and moreover using LaCl_3 in some organic solvent should be evaluated.

Further evidence for the $\text{La}_2\text{O}_3/\text{GO}$ nanocomposites was illuminated by the XPS of the GL2. The survey XPS spectra of GL2 (Figure 3(a)) suggested that the $\text{La}3d$ peaks, C 1s peaks, and O 1s peaks could be found in the nanocomposites. C 1s peak was about 284.77 eV; O 1s peak was about 531.94 eV which can be indexed to O^{2-} in La_2O_3 . And Figure 3(b)

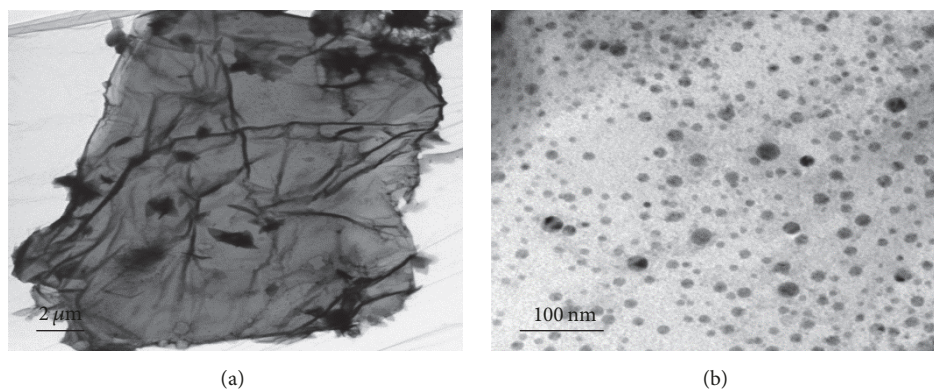
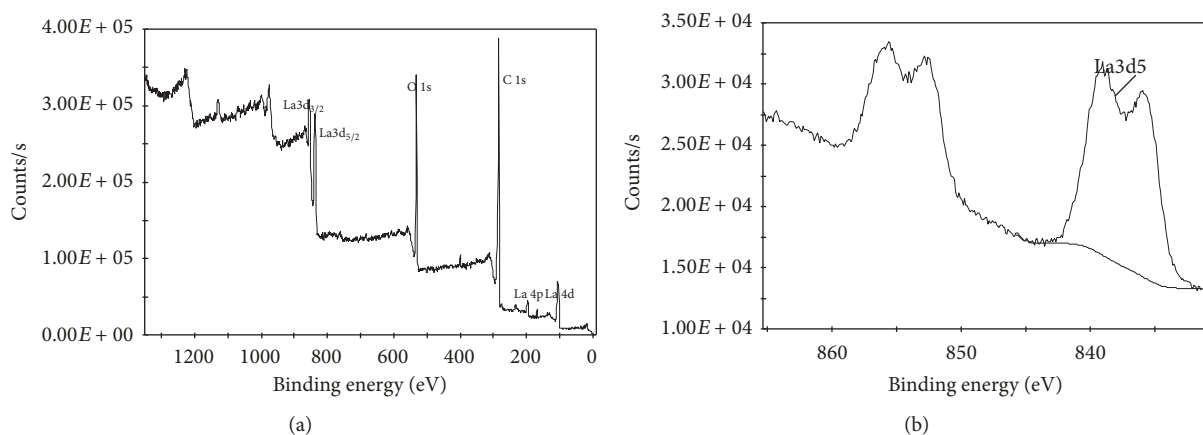


FIGURE 2: TEM images of GL2.

FIGURE 3: XPS spectra of the $\text{La}_2\text{O}_3/\text{GO}$ nanocomposites: (a) survey spectrum; (b) La3d region.

showed the binding energy of $\text{La}3d_{5/2}$ was 838.15 eV. All the above results suggested that $\text{La}_2\text{O}_3/\text{GO}$ nanocomposites were successfully synthesized in DMF. The XRD spectra of $\text{La}_2\text{O}_3/\text{GO}$ nanocomposites were also studied; unfortunately, only a broad peak was observed.

To investigate the application of as-synthesized $\text{La}_2\text{O}_3/\text{GO}$ nanocomposites, the degradation ability for MB, Rh, and MO was studied in pure water. Figure 4 showed the UV-vis spectra of MB, Rh, and MO solutions in presence of GL1, GL2, and GL3 under ultrasound irradiation, respectively. As shown in Figures 4(a), 4(b), and 4(c), the absorbance of MB, Rh, and MO would be decreased in presence of $\text{La}_2\text{O}_3/\text{GO}$ nanocomposites under ultrasound irradiation for 15 min. The decomposition may be due to the reaction of dye molecules with hydroxyl radical which is formed under the ultrasonic irradiation in the presence of $\text{La}_2\text{O}_3/\text{GO}$ nanocomposites [16]. And the degradation efficiency for MB, Rh, and MO was shown in Figure 4(d). The degradation efficiency for MB was about 99.6%, 98.4%, and 99.8% in presence of GL1, GL2, and GL3 after sonication for 15 min, respectively. And degradation efficiency for MO was a little bit lower (76.2%, 79.7%, and 82.5%, resp.), whereas the degradation efficiency for Rh was 49.6%, 63.2%, and 59.6%, respectively.

For comparison, the degradation for MB, Rh, and MO in presence of GO was also studied. There was no obvious change in UV-vis spectra for MO (5.6% efficiency) in presence of GO under ultrasound for 15 min and the degradation efficiency for MB and Rh was only 61.7% and 21.3% in presence of GO, respectively. The above results indicated the as-synthesized $\text{La}_2\text{O}_3/\text{GO}$ nanocomposites were excellent degradation material for some organic dye molecules.

4. Conclusions

In summary, a facile method for the synthesis of $\text{La}_2\text{O}_3/\text{GO}$ nanocomposites has been developed. The $\text{La}_2\text{O}_3/\text{GO}$ nanocomposites could be obtained by simply mixing $\text{LaCl}_3 \cdot 7\text{H}_2\text{O}$ and GO in DMF under reflux condition. The method could be applied to synthesize other rare earth oxides/GO nanocomposites with various morphologies and novel properties. Furthermore, the dye degradation properties were also studied, and the as-synthesized $\text{La}_2\text{O}_3/\text{GO}$ nanocomposites showed excellent degradation efficiency for some organic dye molecules. And, the explicit degradation mechanism is still being investigated.

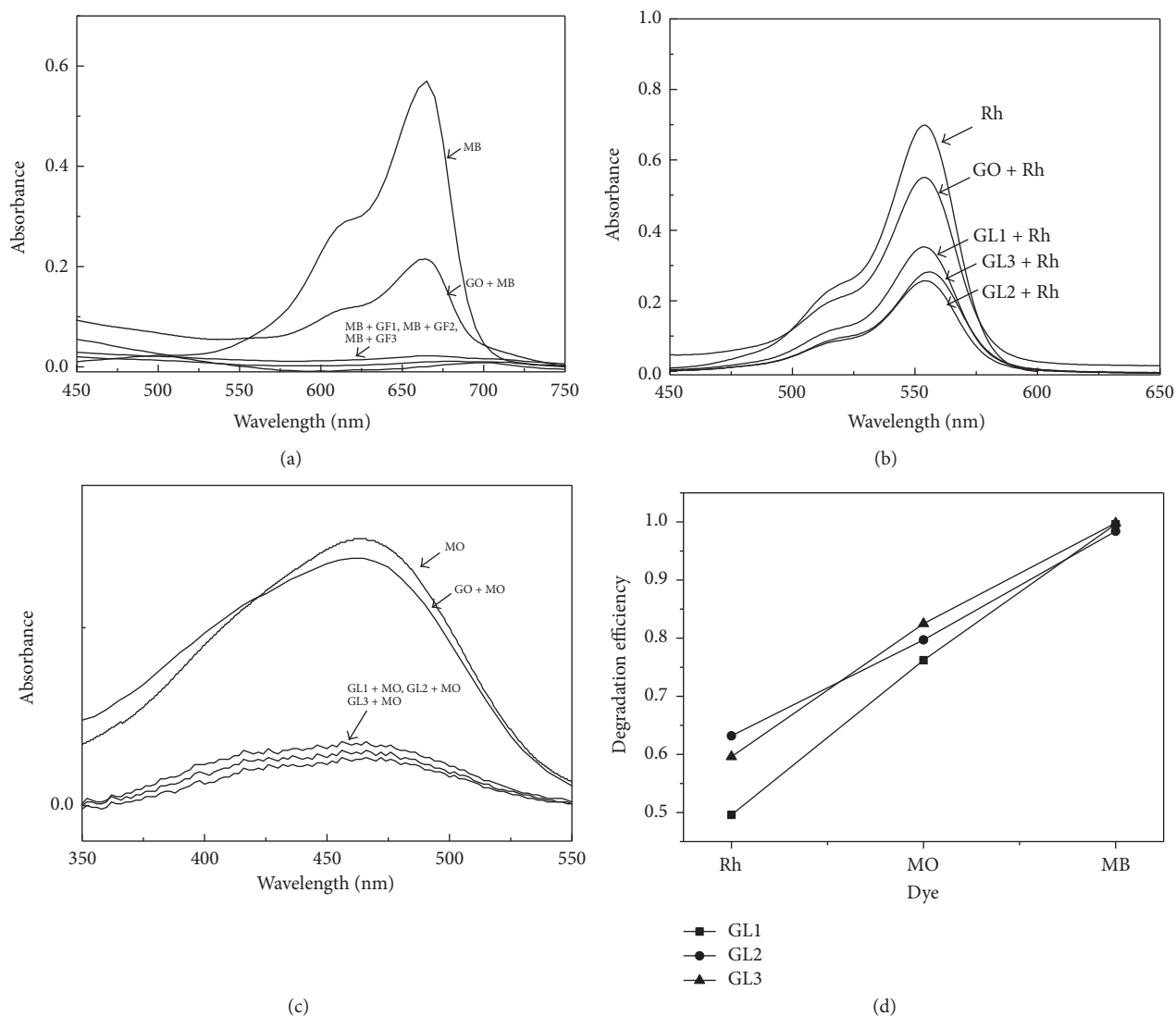


FIGURE 4: UV-vis spectra of (a) MB, (b) Rh, and (c) MO in absence and presence of GL1, GL2, GL3, and GO, respectively, and (d) degradation efficiency of MB, Rh, or MO in presence of GL1, GL2, and GL3, respectively.

Conflicts of Interest

The authors declare that they have no conflicts of interest.

Acknowledgments

This work was supported by Hebei Science and Technology Supporting Program (Program no. 15214404D-2), the Science and Technology Foundation of Universities of Hebei Province (Grant no. ZD2015113), Handan Scientific and Technological Research Development Project (Project no. 1622201049-2), and Foundations of Hebei University of Engineering.

Supplementary Materials

Preparation procedure and TEM images for La_2O_3 without GO; XRD spectra of GL2. Fig. S1: TEM ((a), (b)) and XRD (c)

of as-synthesized solid without GO. Fig. S2: XRD of GL1 (a) and GL2 (b). (Supplementary Materials)

References

- [1] M. Khan, M. N. Tahir, S. F. Adil et al., "Graphene based metal and metal oxide nanocomposites: synthesis, properties and their applications," *Journal of Materials Chemistry A*, vol. 3, no. 37, pp. 18753–18808, 2015.
- [2] F. Cui and X. Zhang, "Electrochemical sensor for epinephrine based on a glassy carbon electrode modified with graphene/gold nanocomposites," *Journal of Electroanalytical Chemistry*, vol. 669, pp. 35–41, 2012.
- [3] J.-D. Qiu, G.-C. Wang, R.-P. Liang, X.-H. Xia, and H.-W. Yu, "Controllable deposition of platinum nanoparticles on graphene as an electrocatalyst for direct methanol fuel cells," *The Journal of Physical Chemistry C*, vol. 115, no. 31, pp. 15639–15645, 2011.

- [4] X. Li, Y. W. He, J. S. Ryu, and S. I. Yang, "Colorimetric detection of Ag ions with graphene oxide in dimethylformamide," *New Journal of Chemistry*, vol. 38, no. 2, pp. 503–506, 2014.
- [5] W. Qu, H. Bao, L. Zhang, and G. Chen, "Far-infrared-assisted preparation of a graphene-nickel nanoparticle hybrid for the enrichment of proteins and peptides," *Chemistry - A European Journal*, vol. 18, no. 49, pp. 15746–15752, 2012.
- [6] L. Ren, S. Huang, W. Fan, and T. Liu, "One-step preparation of hierarchical superparamagnetic iron oxide/graphene composites via hydrothermal method," *Applied Surface Science*, vol. 258, no. 3, pp. 1132–1138, 2011.
- [7] J. Zhang, J. Jiang, and X. S. Zhao, "Synthesis and capacitive properties of manganese oxide nanosheets dispersed on functionalized graphene sheets," *The Journal of Physical Chemistry C*, vol. 115, no. 14, pp. 6448–6454, 2011.
- [8] J. Zhu, S. Chen, H. Zhou, and X. Wang, "Fabrication of a low defect density graphene-nickel hydroxide nanosheet hybrid with enhanced electrochemical performance," *Nano Research*, vol. 5, no. 1, pp. 11–19, 2012.
- [9] Y. Gu, M. Xing, and J. Zhang, "Synthesis and photocatalytic activity of graphene based doped TiO₂ nanocomposites," *Applied Surface Science*, vol. 319, pp. 8–15, 2014.
- [10] N. Wang, Q. Zhang, and W. Chen, "Synthesis and magnetic properties of lanthanum orthovanadate nanorods," *Crystal Research and Technology*, vol. 42, no. 2, pp. 138–142, 2007.
- [11] H.-X. Mai, Y.-W. Zhang, R. Si et al., "High-quality sodium rare-earth fluoride nanocrystals: Controlled synthesis and optical properties," *Journal of the American Chemical Society*, vol. 128, no. 19, pp. 6426–6436, 2006.
- [12] P. Lu, Z. Zeng, C. Li et al., "Room temperature removal of NO by activated carbon fibres loaded with urea and La₂O₃," *Environmental Technology*, vol. 33, no. 9, pp. 1029–1036, 2012.
- [13] S. P. Fricker, "The therapeutic application of lanthanides," *Chemical Society Reviews*, vol. 35, no. 6, pp. 524–533, 2006.
- [14] S. K. Beaumont, G. Kyriakou, and R. M. Lambert, "Identity of the active site in gold nanoparticle-catalyzed sonogashira coupling of phenylacetylene and iodobenzene," *Journal of the American Chemical Society*, vol. 132, no. 35, pp. 12246–12248, 2010.
- [15] M. Chen, C. Huo, Y. Li, and J. Wang, "Selective adsorption and efficient removal of phosphate from aqueous medium with graphene-lanthanum composite," *ACS Sustainable Chemistry & Engineering*, vol. 4, no. 3, pp. 1296–1302, 2016.
- [16] P. Nuengmatcha, S. Chanthai, R. Mahachai, and W.-C. Oh, "Sonocatalytic performance of ZnO/graphene/TiO₂ nanocomposite for degradation of dye pollutants (methylene blue, texbrite BAC-L, texbrite BBU-L and texbrite NFW-L) under ultrasonic irradiation," *Dyes and Pigments*, vol. 134, pp. 487–497, 2016.



Hindawi
Submit your manuscripts at
www.hindawi.com

